Matrix Biology Plus 22 (2024) 100143

Contents lists available at ScienceDirect

Matrix Biology Plus

journal homepage: www.sciencedirect.com/journal/matrix-biology-plus

Laminin-derived peptide, IKVAV, modulates macrophage phenotype through integrin mediation

Aakanksha Jha [a,b], Erika Moore [a,b,*]

[a] J. Crayton Pruitt Family Department of Biomedical Engineering, University of Florida, Gainesville, FL, United States
[b] Fischell Department of Bioengineering, University of Maryland, College Park, MD, United States

ARTICLE INFO

Keywords:
Extracellular matrix
Macrophages
Integrins
ECM-derived peptide
Biomaterials

ABSTRACT

Macrophages are highly plastic immune cells known to exist on a spectrum of phenotypes including pro-inflammatory (M1) or pro-healing (M2). Macrophages interact with extracellular matrix (ECM) ligands, such as fragments of collagen and laminin. Interaction of macrophages with ECM ligands is mediated through integrin receptors. However, the role of ECM ligands in directing macrophage function through integrins is not yet fully understood. Particularly, α2β1 has been implicated in modulating macrophage function, but complexity in mechanisms employed for integrin-ligation especially with laminin-derived peptides makes it challenging to understand macrophage-ECM interactions. We hypothesize that targeting α2β1 through laminin-derived peptide, IKVAV, will modulate macrophage phenotype. In this work we: i) investigated macrophage response to IKVAV in 2D and in a 3D platform, and ii) identified α2β1's role as it pertains to macrophage modulation via IKVAV. Soluble IKVAV treatment significantly reduced M1 markers and increased M2 markers via immunocytochemistry and gene expression. While the 3D ECM-mimicking PEG-IKVAV hydrogels did not have significant effects in modulating macrophage phenotype, we found that macrophage modulation via IKVAV is dependent on the concentration of peptide used and duration of exposure. To investigate integrin-ligand interactions for macrophages, α2β1 signaling was modulated by antagonists and agonists. We observed that blocking α2β1 reduces M1 activation. To understand integrin-ligand interactions and leveraging the therapeutic ability of macrophages in designing immunomodulatory solutions, it is critical to elucidate IKVAV's role in mediating macrophage phenotype.

Introduction

The extracellular matrix (ECM) is a complex network of macromolecules organized specifically in cells and tissues. Along with contributing to the mechanical properties of tissues, the ECM also serves as a reservoir of growth factors and bioactive molecules [1,2]. The ECM has several proteins like collagen, laminin, and fibronectin that have been shown to function as ligands for certain cell surface receptors [3]. Integrins are principal transmembrane receptors used by cells to bind to the ECM [4]. They are bidirectional signaling receptors composed of α and β heterodimers that dictate cell function by acting as bridges between the ECM and the cytoskeleton [5–7]. Integrins have different affinities for diverse ECM ligands or peptide sequences within them [8]. One such ECM ligand is laminin that supports structure and function, and is a major constituent of the basement membrane [9]. While integrins transduce signals into the cell interior on ligand binding, integrins can also regulate their ligand-binding affinity upon receiving intracellular signals. These signals are especially important for immune cell functioning such as for migration through the basement membrane. The complexity in mechanisms employed for integrin-ligation makes it challenging to understand immune cell-ECM interactions. Defining ligand-receptor interactions to direct cell function can revolutionize the understanding of macromolecular aspects in immune engineering techniques.

Macrophages are innate immune cells that participate in inflammatory responses, phagocytosing foreign bodies, producing regulatory cytokines, and ECM remodelling [10–13]. Due to their diverse functions, macrophages are considered to exist on a spectrum of functional activation states or phenotypes such as pro-inflammatory (M1) or anti-inflammatory (M2) [14–16]. While traditionally investigated through cytokine stimulation, macrophage phenotypic states are dictated by physical properties of the ECM and integrin-ligand interactions [17]. For

* Corresponding author.
E-mail address: emt@umd.edu (E. Moore).

https://doi.org/10.1016/j.mbplus.2024.100143
Received 7 November 2023; Received in revised form 16 January 2024; Accepted 6 February 2024
Available online 15 February 2024

example, the 3D structure of the ECM plays an important role in the macrophage phenotypic modulatory process. Exposure of macrophages to 3D matrices without ECM properties have encouraged M1 activation whereas ECM scaffolds or ECM-mimicking materials have encouraged M2 activation [18,19]. Macrophages interact with basement membranes and other components of the ECM at specific times during their ontogeny and differentiation, as well as in response to appropriate physiological stimuli [20]. During tissue inflammation, macrophages utilize laminin receptors to bind to vascular basement membranes via integrins and interact with microbes at sites of inflammation [21]. Uncontrolled or persistent inflammation in macrophages by sustenance of the M1 phenotype may lead to suboptimal ECM composition preventing regeneration [22,23]. Since integrins also regulate macrophage function, it is important to leverage integrin mediation and promote healing by reducing M1 activation or promoting M2 activation. Investigating the intricate interactions between macrophages and their ECM is crucial for developing effective tools and interventions to modulate macrophage function and harness their therapeutic potential.

Particularly, integrin α2β1 (also known as very late activating antigen (VLA)-2) has been implicated in controlling macrophage phenotype [24,25]. Recent studies demonstrate that α2β1 promotes wound healing by upregulating ECM remodeling for regeneration and increasing macrophage recruitment [25,26]. As a receptor that regulates macrophage activation state, α2β1 is an attractive target for therapeutic strategies to promote healing. Recent findings suggest that α2β1 is a mutual receptor between laminin and collagen for certain stromal cells such as endothelial cells (ECs) [27,28]. Particularly, α2β1′s role as a receptor for collagen was demonstrated in our previous work wherein a collagen-derived peptide DGEA reduced M1 activation by blocking α2β1 [29]. Whether α2β1 is also a common receptor between collagen and laminin in macrophages is unknown. It is important to investigate macrophage response to laminin due to its potential modulatory effects on macrophages via α2β1 and its abundance in the ECM.

Ile-Lys-Val-Ala-Val (IKVAV) is a laminin-derived peptide that is known for its pro-angiogenic abilities in other stromal cells, but its role in macrophages is not yet explored [30,31]. IKVAV, discovered in 1989, has been traditionally used to promote angiogenesis, neurite formation, regeneration of neuronal stem cells, along with spreading and migration of cells [30,32,33]. However, to our knowledge, IKVAV has not been evaluated as a macrophage manipulating peptide. It is important to define the receptor mechanisms used by macrophages to interact with laminin. Additionally, investigating whether integrin signaling is a crucial player that controls macrophage activation are key areas that merit investigation.

This work aims to investigate macrophage response to IKVAV, and therefore understand α2β1 mechanisms as an aspect of macrophage-IKVAV interactions. We postulate that due to IKVAV binding with integrin α2β1, IKVAV will reduce M1 activation and increase M2 activation. We utilized the IKVAV peptide sequence in 2D and in a 3D platform. The 2D studies were performed to establish relations between macrophages and α2β1 with IKVAV exposure. To better capture 3D interactions, we designed an ECM-mimicking hydrogel using poly (ethylene glycol) (PEG). To mimic the functions of cell adhesion and migration, cell-adhesive and enzyme-cleavable peptides along with IKVAV were covalently conjugated to PEG to form the hydrogel. The results obtained demonstrate that the ability of macrophages to adapt an M1 or M2 phenotype is dependent on the concentration of IKVAV and duration of exposure. Soluble IKVAV treatment in 2D experiments reduced M1 markers and increased M2 markers via gene expression assays and immunocytochemistry. PEG-IKVAV hydrogels were efficient in preventing the activation of M1 macrophages but did not have significant effects in modulating macrophage phenotype. We also investigated integrin α2β1 and IKVAV interactions governing macrophage function. To investigate integrin-ligand interactions in macrophage manipulation, we modulated α2β1 signaling. We observed that blocking α2β1 signaling reduces M1 activation. We therefore demonstrate IKVAV's role as a macrophage manipulating peptide and highlight the importance of α2β1 signaling as a potential target in designing immunomodulatory therapeutics.

Results and discussion

The goal of this work was to analyze laminin-derived peptide IKVAV's role on macrophage manipulation and better define the impact of α2β1 in macrophage phenotype modulation. We postulate that due to blocking α2β1 binding sites, IKVAV may reduce M1 activation. Since macrophage phenotypic switches may be synchronized, an increase in M2 activation may also be expected. Assessing the capacity of IKVAV in manipulating macrophage phenotype and identifying if α2β1 signaling affects phenotypic state is pertinent to better understanding ECM ligand-integrin receptor interactions.

IKVAV reduces M1 activation in 2D cultures of macrophages

A dose-dependent response experiment was conducted to determine the appropriate concentration for IKVAV treatment on macrophages (**Fig S-1**). Macrophages were stained for M1 marker inducible nitric oxide synthase (iNOS) and M2 marker arginase-1 (Arg-1) with and without IKVAV treatment. Because 3 mM IKVAV caused the highest magnitude of reduction in iNOS expression, it was chosen as the experimental concentration for reducing M1 activation and for all subsequent experiments.

Murine macrophages were first utilized to define macrophage response to IKVAV. Fig. 1 represents murine M0, M1, and M2 macrophages treated with and without 3 mM IKVAV as mean fluorescence intensities (MFI) of iNOS and Arg-1 expression. The violin charts are represented as superplots of the data wherein the larger dots are the means. IKVAV treatment significantly reduced iNOS expression from 82.13 ± 23.97 arbitrary units (a.u.) to 50.95 ± 7.3 a.u. for M1 macrophages. The iNOS expression for M0 and M2 macrophages had no significant differences with IKVAV treatment (Fig. 1**a,b**).

IKVAV was also shown to increase Arg-1 expression in M0 and M1 macrophages (Fig. 1**b**). IKVAV treated M0 macrophages expressed Arg-1 at 63.62 ± 2.74 a.u. compared to 37.92 ± 1.75 a.u. without IKVAV. M1 macrophages had an increase of 4.74 a.u. from 39.73 ± 5.48 a.u. without IKVAV to 44.48 ± 6.21 a.u. with IKVAV treatment. The differences of Arg-1 expression between M2 IKVAV treated and non IKVAV treated macrophages was minimal i.e., 0.61 a.u MFI. Arg-1 expression levels were influenced following IKVAV treatment in M0 and M1 groups. While the magnitude of expression difference was less than iNOS MFI, the trends indicate that IKVAV treatment may reduce the inflammatory phenotype in M1 stimulated macrophages and increase an M2 phenotype in M0 macrophages. Differences in cell density between murine M0 and M1/M2 macrophages were observed (**Fig S-2**). Disparity in cell counts could be due to fewer sites of adhesion by interrupted integrin-ligation, or M1 macrophages having low motility [34,35].

To assess IKVAV influence on human macrophages, experiments were also conducted in human PBMC-derived macrophages (Fig. 2). Since IKVAV had a muted response on Arg-1 expression for M2-treated murine macrophages (Fig. 1**b**), human macrophages were only stained for iNOS with M0 and M1 macrophages. IKVAV treatment did not significantly change iNOS expression for M0 macrophages. For M1 macrophages, iNOS expression significantly decreased with IKVAV treatment. The mean of MFI was 196.5 ± 27.77 a.u. in M1 macrophages without IKVAV treatment which reduced to 177.8 ± 30.79 a.u. with IKVAV treatment.

The data in Figs. 1 and 2 are representative of IKVAV reducing iNOS in previously stimulated murine and human M1 macrophages. iNOS is commonly used as a canonical M1 marker due to its abundant presence on activation of inflammatory cells [36,37]. High levels of iNOS induce nitric oxide (NO) production which in combination with reactive oxygen species (ROS) mediates potent killing activity of macrophages towards

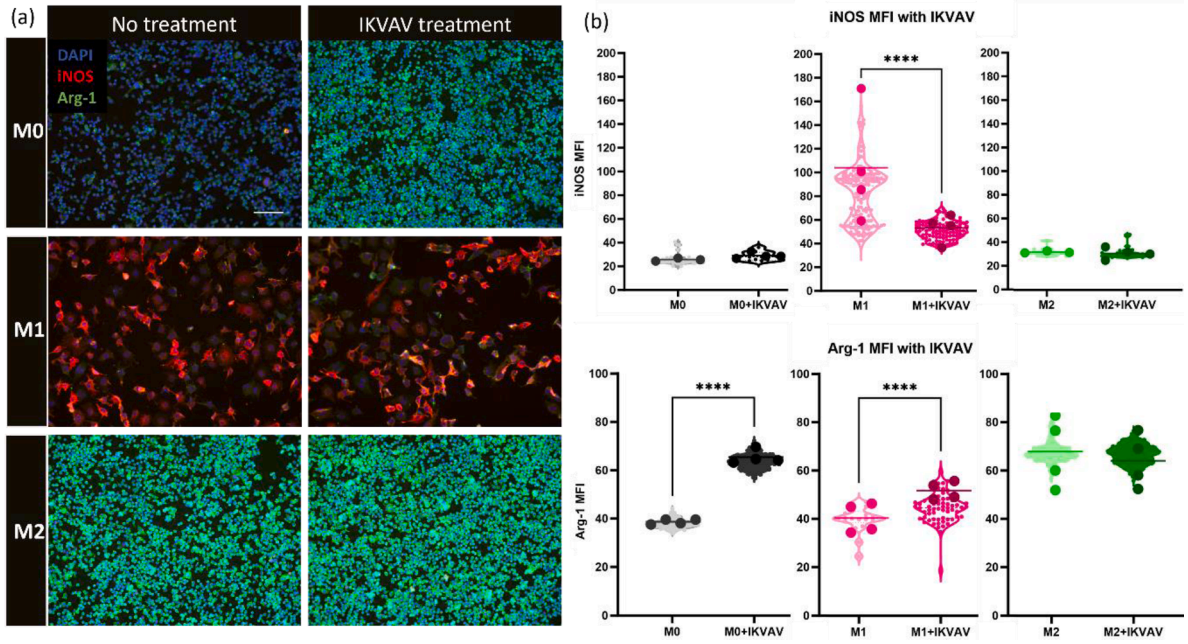

Fig. 1. IKVAV treatment for 48 h reduces iNOS and increases Arg-1 expression in murine M1 macrophages. (a) Arg-1 and iNOS immunofluorescent stained images of IKVAV treated and untreated macrophages polarized to M1 and M2 (scale = 50 mm). (b) Statistical quantification of iNOS and Arg-1 expression via mean fluorescence intensity (MFI). Data are displayed with violin plots where each dot represents the MFI value of a cell, and the larger dots represent superplots of the means. Significance assessed by one-way ANOVA with Tukey's post-hoc tests among IKVAV treated and untreated groups (n = 4; ****$p < 0.0001$).

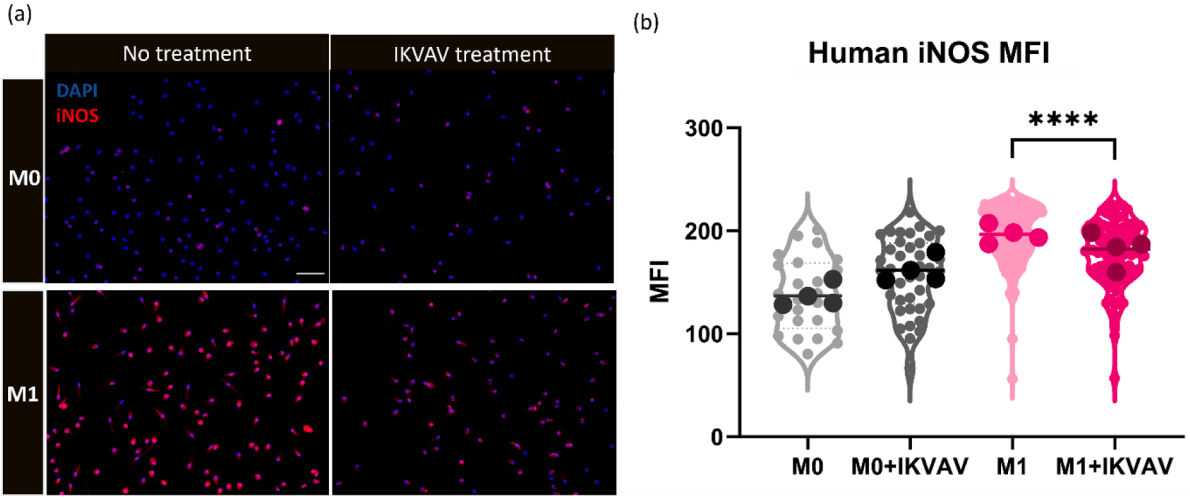

Fig. 2. IKVAV treatment reduces iNOS expression in human M1. (a) Immunofluorescent images of DAPI (blue; nuclear stain) and iNOS (red; M1 stain) IKVAV treated and untreated macrophages (scale = 50 mm). (b) Statistical quantification of iNOS expression via MFI. Data are displayed with violin plots where each dot represents the MFI of a cell. The larger dots are superplots of the means of the data. The mean standard deviation values are reported. One-way ANOVA with Tukey's post-hoc among IKVAV treated and untreated groups of macrophages was utilized to assess significance (n = 4; ****$p < 0.0001$). (For interpretation of the references to color in this figure legend, the reader is referred to the web version of this article.)

intracellular pathogens. Therefore, IKVAV reducing iNOS expression may signify a less inflammatory macrophage phenotype. The reduction of iNOS expression with IKVAV treated M1 macrophages as seen in murine macrophages was also sustained in human macrophages. Similarly, IKVAV treatment increasing M1 macrophage Arg-1 expression (Fig. 1**b**) may reflect a shift to a pro-healing or anti-inflammatory function, given the critical role of Arg-1 in tissue repair processes and suppressing inflammation [38–40].

This work introduces IKVAV as a macrophage manipulating peptide. IKVAV has been a popular peptide for promoting angiogenesis with ECs and in regeneration of neuronal tissue [32,33,41]. Although IKVAV was recently utilized for therapeutic purposes in spinal cord injuries [42], it has never been used, to our knowledge, for mechanistic understanding as it pertains to macrophage modulation. The variations in iNOS and Arg-1 expression in M1 macrophages can be better understood by analyzing the genetic profile of IKVAV treated macrophages.

IKVAV treatment reduces pro-inflammatory markers and increases anti-inflammatory markers via gene expression

We utilized Nanostring gene expression techniques to identify differentially expressed genes and signaling pathways that are affected by IKVAV treatment on human macrophages. No prior studies have evaluated the gene expression profile of human macrophages in

response to IKVAV treatment. The volcano plot of differentially expressed genes with no IKVAV treatment as baseline is represented with upregulated genes in blue and downregulated genes in red (Fig. 3**a**). Specifically, the volcano plot represents all macrophage treatments with IKVAV, including M0, M1, and M2, versus no IKVAV treatment.

IKVAV treatment upregulated genes associated with anti-inflammatory responses, including vascular endothelial growth factor A (VEGFA), migration inhibitory factor (MIF), chemokine receptor 4 (CXCR4), insulin receptor (INSR), and S100 Calcium Binding Protein A10 (S100A10) (Fig. 3**a**). For example, elimination of apoptotic cells is crucial to resolve inflammation and promote healing [43]. VEGFA is a growth factor for ECs and inhibitor of apoptosis [44–46]. Similarly, MIF and INSR reduce apoptosis in macrophages [47,48]. An upregulation of these genes signifies inflammation resolution in macrophage function.

IKVAV downregulated expression of genes associated with pro-inflammatory responses including lipoprotein lipase (LPL), formyl peptide receptor 2 (FPR2), mitogen activated protein kinase 13 (MAPK13), and C-C motif chemokine receptor-like 2 (CCRL2) (Fig. 3**a**). MAPK13 is involved in the production of inflammatory mediators such as tumor necrosis factor alpha (TNFα) [49]. Downregulation of MAPK13 suggests that IKVAV induces a less inflammatory environment. Similarly, CCRL2 and LPL increase macrophage inflammation capacity on LPS-activation hence their downregulation is beneficial to inhibiting macrophage inflammation [50,51]. The highest log2 fold change value was observed in FPR2 downregulation. This downregulation can be associated with phenotypic switching of macrophages wherein the reduction of FPR2 allows anti-inflammatory function of macrophages [52]. Therefore, the downregulation of these genes with IKVAV signifies a reduction in inflammatory gene expression.

To compare normalized log2 fold change values of specific genes related to M1 (Fig. 3**b**) and M2 macrophages (Fig. 3**c**), bar charts were plotted for IKVAV treated M1 and M2 macrophages versus no IKVAV treatment. These bar graphs demonstrate changes to genes that are commonly associated with the M1 and M2 phenotypes. Genes related to M1 macrophages represented are TNF, toll-like receptor (TLR2), CD86, hypoxia inducible factor 1 alpha (HIF1A), and CCL2. All the listed genes are related to pro-inflammatory responses and were reduced with IKVAV treatment, which signifies that IKVAV induces a less inflammatory macrophage phenotype.

M2 related anti-inflammatory genes were upregulated with IKVAV treatment, including MMP9, gelsolin (GSN), tumor growth factor beta (TGFB1), NF-kappa-B inhibitor zeta (NFkBIZ), TLR6, etc. NFkBIZ upregulation induces the expression of anti-inflammatory cytokine IL-10 [53]. GSN promotes wound healing by resolving inflammation in *in vitro* wound models [54]. Therefore, an increase in expression of both NFkBIZ and GSN signifies an inhibition of inflammatory M1 macrophages and promotion of M2 macrophages.

Particularly noteworthy for ECM remodeling is MMP-9, a matrix remodeling enzyme shown to be upregulated in M2 macrophages. Literature also suggests that MMP-9 is upregulated with IKVAV treatment [32,55]. Fig. 3**c** demonstrates that IKVAV treatment increases expression of MMP-9 in M2 macrophages. These results suggest that IKVAV promotes ECM remodeling and M2 activation. Additionally, S100A10 was amongst the upregulated genes with IKVAV treatment (Fig. 3**a**). S100A10 activates MMPs and is released after activation of macrophages [56], alluding to IKVAV being more potent in dictating macrophage function when they are already phenotypically differentiated.

Utilizing Nanostring gene expression with human macrophages provides a more detailed analysis of the array of genes being up- or down-regulated. The pathways being affected can also be inferred from these studies. RT-qPCR was also conducted to analyze gene expression of murine macrophages (**Fig S-3**). While no statistical significance was observed in IKVAV treated macrophages, some interesting trends are described in the supplemental information such as an increase in IL-10 expression with IKVAV treated M2 macrophages. IKVAV treatment significantly downregulates expression of M1 related or pro-inflammatory genes and upregulates expression of M2 related or anti-inflammatory genes, including genes involved in ECM remodeling.

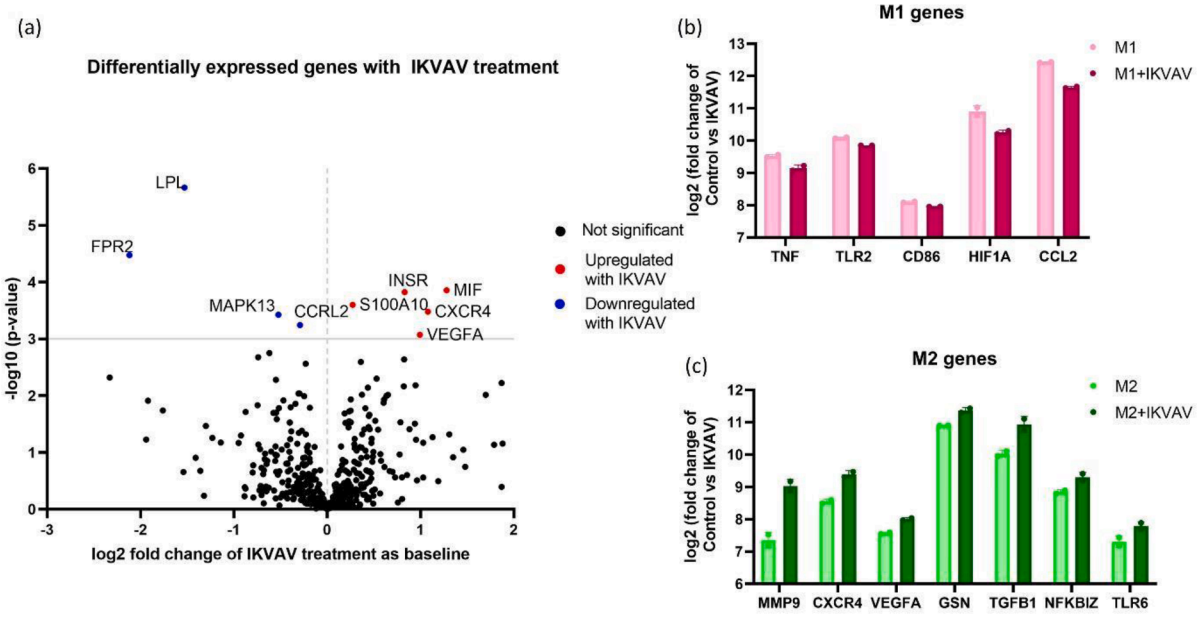

Fig. 3. Nanostring gene expression demonstrates reduction of pro-inflammatory markers and upregulation of anti-inflammatory markers post IKVAV treatment in human macrophages. (a) Volcano plot exhibiting differentially expressed genes amongst M0, M1, and M2 macrophages with no IKVAV treatment as baseline. Red dots signify upregulated genes with IKVAV treatment. Blue dots signify downregulated genes with IKVAV treatment. Threshold was set at corrected p value < 0.50. (b) Bar plots with M1 (pro-inflammatory) associated genes and (c) M2 (anti-inflammatory) associated genes. ($n = 2$ biological replicates and $n = 4$ technical replicates). (For interpretation of the references to color in this figure legend, the reader is referred to the web version of this article.)

PEG-IKVAV at 3 mM in hydrogels does not inform macrophage function in 3D

To understand how a 3D ECM-mimicking environment would alter macrophage function with IKVAV, murine macrophages were encapsulated in control and 3 mM PEG-IKVAV hydrogels (Fig. 4**a**). The average MFI is represented as violin plots within which each dot is a cell expressing iNOS or Arg-1, and the larger dots are the means of the data displayed as superplots. (Fig. 4**b**).

In comparison to IKVAV treatment in a 2D system (Figs. 1 and 2), IKVAV conjugation to 3D PEG hydrogels did not as robustly alter macrophage iNOS and Arg-1 expression (Fig. 4). The MFI of iNOS expression is the highest in M1 macrophages at 181 ± 19.64 a.u. Even though iNOS expression for PEG-IKVAV encapsulated M1 macrophages is lower at 179.1 ± 32.57 a.u., the difference of means is only 1.89 a.u. (Fig. 4**b**). Therefore, PEG-IKVAV encapsulated M1 macrophages displayed a trend of reducing iNOS expression, albeit non-significant (Fig. 4**b**).

There is a significant reduction of M0 macrophage iNOS expression with PEG-IKVAV gels. M0 macrophages express 95.50 ± 29.20 a.u. iNOS in PEG-IKVAV gels compared to 132.3 ± 31.56 a.u. in control gels. There are no significant differences in iNOS expression for M2 macrophages. Arg-1 expression did not exhibit significant differences regardless of macrophage phenotype or hydrogel composition. Fewer superplots of the data (3) observed for Arg-1 expression (Fig. 4**b)** represents that there are lesser cells positively expressing Arg-1 as compared to iNOS. DAPI counts were not affected by encapsulation of macrophages in control and PEG-IKVAV hydrogels (**Fig S-4**).

To investigate human macrophage response to PEG-IKVAV hydrogels, human monocyte-derived macrophages were encapsulated in control and 3 mM PEG-IKVAV hydrogels (Fig. 5). As with murine macrophages, M0 macrophages encapsulated in PEG-IKVAV hydrogels demonstrated a significant reduction in iNOS expression from 153.6 ± 42.16 a.u. in control gels to 73.88 ± 8.68 a.u. in PEG-IKVAV gels. M1 macrophages showed no significant differences (Fig. 5**b**). The reduction of iNOS in M0 macrophages encapsulated in PEG-IKVAV hydrogels highlights IKVAV's role as an inflammation reducing peptide.

The data represent that IKVAV may be facilitating phenotypic shifts with 2D treatment for M0 and M1 macrophages, but the 3D condition shows fewer substantial effects that appear primarily in M1 macrophages. Based on prior work with collagen-derived peptide DGEA, similar concentrations produced comparable results in 2D and 3D [29,57]. However, due to 3 mM IKVAV not producing similar trends in 3D as it did with 2D, optimization for IKVAV concentration must occur independently in 2D and 3D. This optimization was not necessary for DGEA which elucidates differences in integrin-ligand interactions for peptides despite using the same receptor. Therefore, the 3D conditions may be improved by altering concentration of IKVAV or duration of time exposure, to better replicate *in vivo* conditions and avail a more significant shift in macrophage phenotype in the PEG-IKVAV gels.

Another area of investigation for the current hydrogel might be competitive binding of macrophages to the adhesion sites provided by peptide components in the 3D system. For example, RGD is commonly accepted as a general integrin-binding motif on target ligands like fibronectin, laminin, and fibrinogen [58,59]. However, individual integrins can also recognize other protein-specific motifs, in this case IKVAV. It has been shown that the combination of RGDS and IKVAV enhances cell adhesion for mesenchymal stem cells and dorsal root ganglions in a time and concentration dependent manner [41,60]. However, it should be noted that this effect may not hold true for macrophages due to potential differences in their integrin receptors and intracellular mechanisms. Alternating peptides for cell-adhesion or

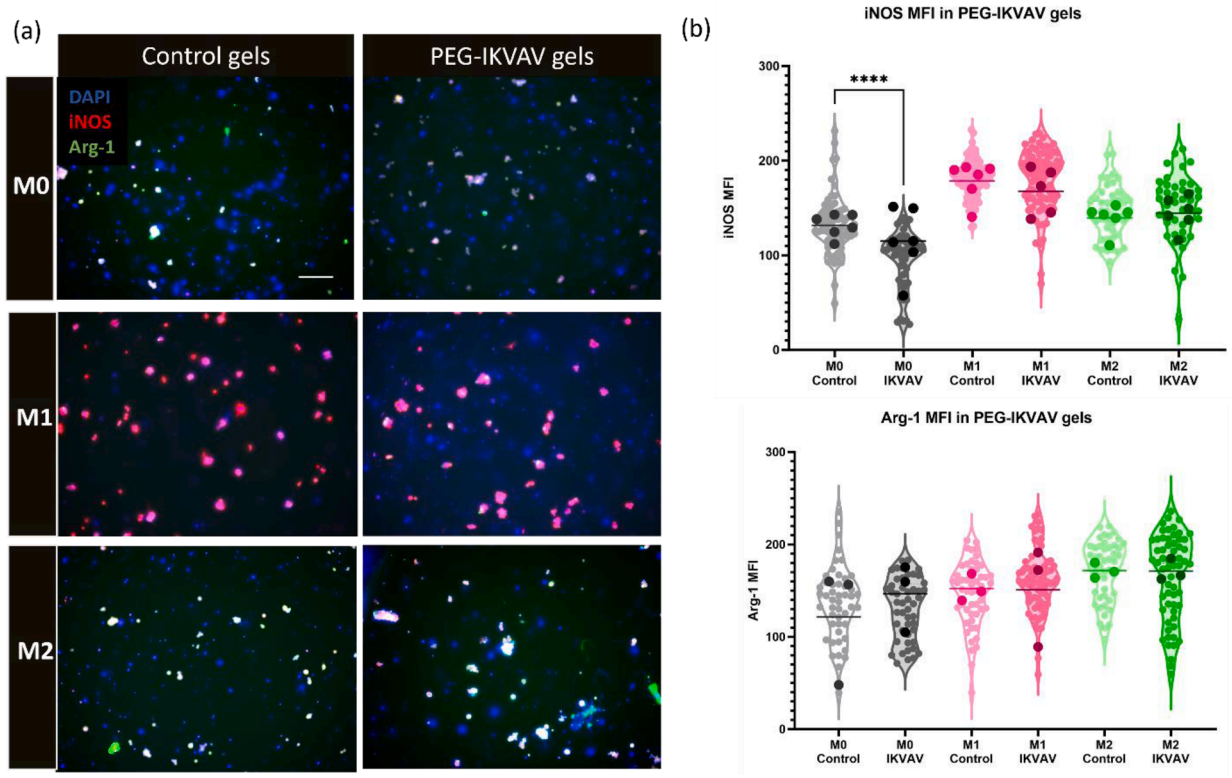

Fig. 4. Murine macrophages encapsulated in 3 mM PEG-IKVAV hydrogels do not display any significant changes in iNOS expression. (a) Immunofluorescent stained images of M0, M1, and M2 macrophages encapsulated in control and PEG-IKVAV hydrogels (scale = 50 mm). (b) Statistical quantification of iNOS and Arg-1 expression via MFI. Data are displayed as violin plots and each smaller, lighter colored dot represents the MFI value of a cell, while larger darker colored dots are means of the data displayed as superplots. One-way ANOVA with Tukey's post-hoc was utilized to compare significance between control and PEG-IKVAV macrophages. (n = 6; ****p < 0.0001).

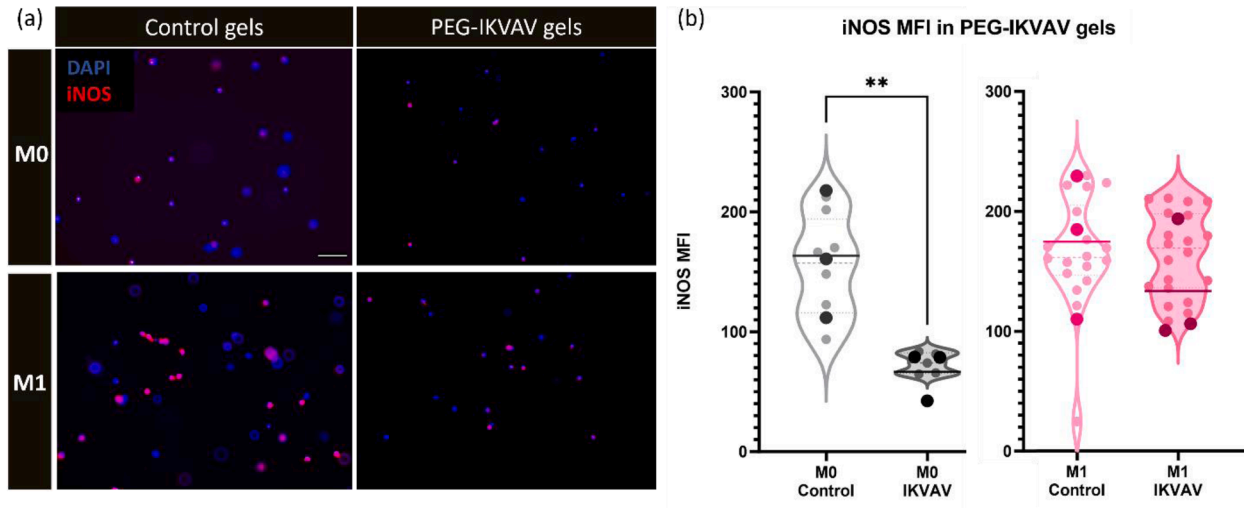

Fig. 5. PEG-IKVAV (3 mM) encapsulated human macrophages do not display significant changes in iNOS expression for M1. (a) Immunofluorescent stained images of M0 and M1 macrophages encapsulated in control and PEG-IKVAV hydrogels (scale = 50 mm). (b) Statistical quantification of iNOS expression via MFI. Data are displayed as violin plots and each small dot represents the MFI value of a cell, while the larger dots are superplots of the means of the data. One-way ANOVA with Tukey's post-hoc was utilized to compare significance between control and PEG-IKVAV macrophages. (n = 6; **p < 0.01).

reducing the concentration of RGDS may modify adhesion sites being presented to macrophages encapsulated in the hydrogel. Importantly, PEG-IKVAV is not increasing M1 activation at the current concentration, which may have beneficial ramifications on its role as a macrophage inflammation reducing peptide.

Blocking α2β1 reduces iNOS expression in M1 macrophages

To investigate if changes in macrophage phenotype were mediated by direct binding or blocking of IKVAV to integrin α2β1, we used antagonists to competitively block the interaction between integrin and IKVAV, or agonists to activate integrin α2β1. BTT-3033, a sulfonamide derivative, was chosen as the antagonist due to its potency in blocking α2β1 [61,62]. Integrin influences cell function depending on whether the integrin-ligand affinity state is low, intermediate, or high [4,63]. BTT-3033 is a low-affinity antagonist. Due to its high efficacy in blocking adhesion sites, BTT-3033 causes apoptosis at higher concentrations. With dose response experiments (**Fig S-5**), a concentration of 2 μM BTT-3033 was deduced as appropriate for blocking α2β1 without significant cell death. The duration of IKVAV exposure was 48 h for 2D soluble treatment (Fig. 1) compared to 24 h only for antagonist experiments (Fig. 6), to avoid significant apoptosis. **Fig S-6** depicts differences

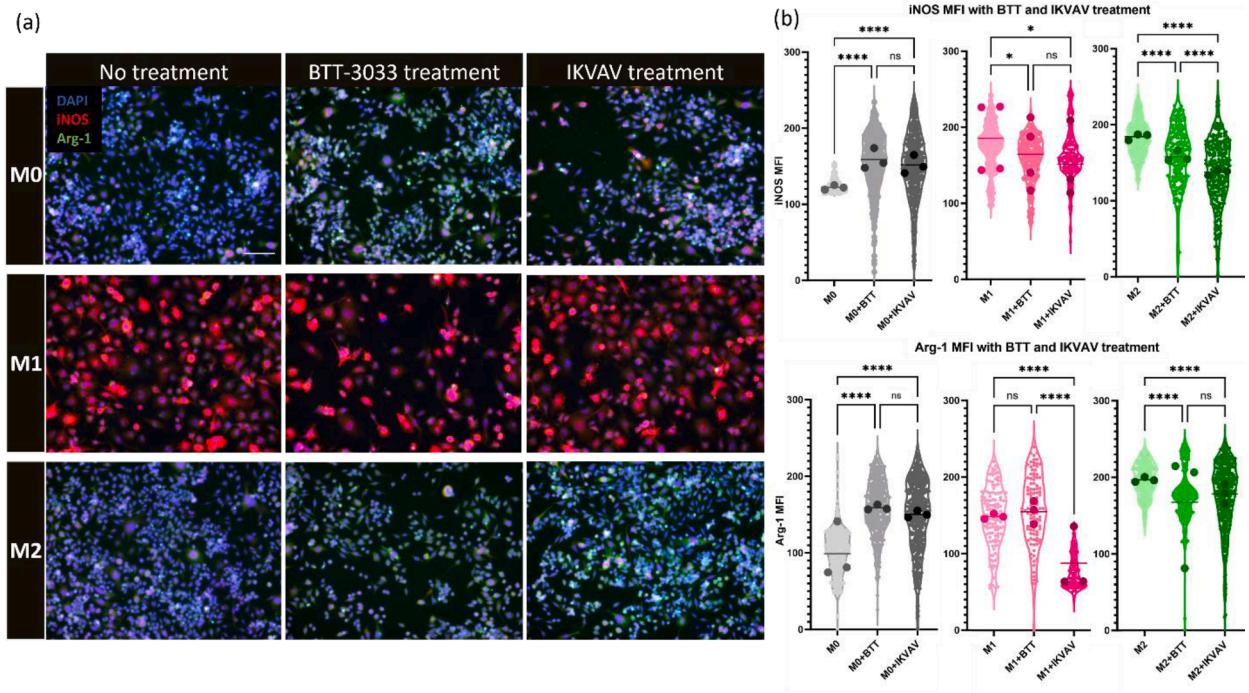

Fig. 6. Blocking integrin α2β1 via antagonist BTT-3033 for 24 h reduced iNOS expression in M1 macrophages. (a) Immunofluorescent stained images of M0, M1, and M2 macrophages with BTT-3033 (2 μM) treatment, and IKVAV (3 mM) treatment (scale = 50 mm). (b) Statistical quantification of iNOS and Arg-1 expression via MFI. Data are displayed as violin plots and each small dot represents the MFI value of a cell, while the larger dots are superplots of the means. One-way ANOVA with tukey's post-hoc tests compared significance between BTT-3033 and IKVAV treated groups. (n = 3; *p < 0.05, ****p < 0.0001).

in DAPI cell counts between all treatment conditions.

BTT-3033 treatment significantly reduced iNOS expression in M1 macrophages to levels that did not significantly differ from that of IKVAV treatment (Fig. 6). The MFI of iNOS expression in M1 macrophages was 175.6 ± 29.88 a.u which reduced to 158.6 ± 30.06 a.u. with BTT-3033 treatment. IKVAV treated M1 macrophages also displayed a reduced MFI of 161.4 ± 34.34 a.u (Fig. 6**b**). For M0 macrophages iNOS expression significantly increased with BTT-3033 treatment to levels comparable with IKVAV treatment. This suggests that integrin α2β1 is more effective at reducing iNOS and manipulating macrophage phenotype when the macrophages are already activated to M1.

M2 macrophages reduced iNOS expression with BTT-3033 treatment, with a significantly larger reduction with IKVAV treatment (Fig. 6**b**). M2 macrophages do not traditionally express iNOS but IKVAV treatment further reduced the iNOS expression, corroborating the deduction that α2β1 is more effective in dictating macrophage phenotype after M1/M2 stimulation.

BTT-3033 treatment increased Arg-1 expression for M0 macrophages, with a similar increase with IKVAV treatment. Due to similar trends between BTT-3033 and IKVAV treatment, it can be suggested that IKVAV may block α2β1 to some extent. The observed reduction in cell numbers of M0 IKVAV treated and untreated macrophages could be further explained due to the blockage of adhesion sites provided by α2β1.

M1 macrophages displayed a non-significant increase in Arg-1 expression with BTT-3033 treatment, but a significant decrease with IKVAV treatment (Fig. 6**b**). Arg-1 expression in M2 macrophages was reduced with BTT-3033 treatment to an extent that did not significantly differ from that of IKVAV treatment. As with the M1 activation state with iNOS, IKVAV plays a significant role in dictating M2 activation state with respect to Arg-1 at 24 h, before and after M1/M2 stimulation.

Notably, M1 macrophages increase Arg-1 expression with IKVAV exposure in Fig. 1 but not in Fig. 5. This difference could be attributed to the duration of IKVAV exposure on macrophages wherein longer exposure times cause more significant changes in Arg-1 expression. Additionally, all M1 and M2 media was removed before treating with BTT-3033. This further suggests that IKVAV may be more effective in altering macrophage phenotype when already in an activated state.

These data imply that blocking α2β1 inhibits M1 activation by reducing iNOS expression. IKVAV is known to be bound through combinations of α3β1, α4β1, and α6β1 [64,65]. However, it was not established if IKVAV interacts with α2β1. Since IKVAV treatment displays a similar trend as BTT-3033 in iNOS reduction, it can be implied that IKVAV may partially block α2β1, but this area needs more investigation. Previous work has emphasized the role of collagen-derived peptide DGEA [29] in inhibiting M1 inflammation by reducing iNOS expression. To confirm the role of integrin α2β1, a study was also conducted with the antagonist BTT-3033 with and without DGEA (**Fig S-5**). The trends seen in **Fig S-5** and Fig. 6 highlight similar response to DGEA in that it reduces iNOS expression in M1 macrophages. We hypothesize that similarities in response to the integrin antagonist, DGEA, and IKVAV directly relate to integrin α2β1.

Nonetheless, it appears that the areas of interaction between the IKVAV sequence and α2β1 may not entirely coincide, hinting at distinct signaling mechanisms resulting from the sequestration of ECM fragments. Peptides derived from different chains or regions of the laminin molecule have varying biological effects. For example, contrary to IKVAV derived from the alpha chain, YIGSR derived from the beta chain short arm is traditionally used to reduce angiogenesis and prevent tumor metastasis [55]. Another study utilized a peptide derived from the alpha-1 chain of laminin and observed alterations with MMP-9 expression in murine macrophages. Intact laminin or another peptide derived from the beta-1 chain had no effect on MMP expression [66]. Therefore, altering the concentration of IKVAV within the 3D system may show increased efficacy in blocking α2β1 thereby yielding disparate outcomes compared to the current findings.

Activating α2β1 does not modulate macrophage phenotype

To assess how activation of α2β1 dictates macrophage function, we chose a high-affinity agonist TS2/16. TS2/16 is a monoclonal antibody chosen for its potency in binding with the integrin receptor leading to the activation of α2β1 [4,63,67].

Activation of α2β1 may not affect macrophages that are polarized to M1, since iNOS expression remained unaffected in M1 stimulated macrophages in our studies (Fig. 7). Trends suggest that activating α2β1 may promote inflammation by increasing iNOS expression in M0 although absence of statistical significance may indicate that α2β1 activation also does not dictate the response of non-polarized M0 (Fig. 7). M2 macrophages displayed a significant increase in iNOS expression with TS2/16 treatment. There were no significant differences observed in Arg-1 expression of all macrophage phenotypes. **Fig S-7** depicts differences in DAPI counts between M0, M1, M2 macrophages with TS2/16 and IKVAV treatment.

Based on the findings depicted in Figs. 6 and 7, it can be stated that blocking α2β1 has an impact on macrophage phenotype irrespective of their activation state. However, activating α2β1 does not seem to influence the phenotype of polarized macrophages except increasing iNOS expression in M2 macrophages. Additionally, IKVAV manipulation of macrophage phenotype may be time dependent. We acknowledge that the time difference between Figs. 1 and 6 shows alternate effects of M0 response to IKVAV. However, due to the significant apoptotic reaction observed on BTT-3033 exposure with prolonged duration times exceeding 24 h, all agonist/antagonist experiments involving macrophages were specifically designed to limit the treatment duration to 24 h for TS2/16, BTT-3033, and IKVAV. In contrast, previous studies utilized a 48 h treatment period for IKVAV. Therefore, IKVAV can be a macrophage manipulating peptide based on the duration of exposure.

The correlation between IKVAV's efficiency with time can be observed in Figs. 1 and 7. In the 2D TS2/16 experiments, IKVAV treatment was similar to untreated groups for all macrophage phenotypic states (Fig. 7), except M2. For M0 macrophages MFI of iNOS expression with IKVAV treatment was 124.9 ± 54.41 a.u., for M1 macrophages MFI was 182.9 ± 41.50 a.u., and for M2 macrophages it was substantially higher than untreated M2 at 143.6 ± 53.75 a.u. This is different from the data represented in Fig. 1 with 2D soluble IKVAV treatment suggesting that manipulation with IKVAV is time dependent. There has also been a correlation depicted in the adherence of macrophages to laminin substrata with time. Herein, macrophages acquired the capacity to bind to a substratum of laminin *in vitro*. This capacity increased with time showing a time-dependent up-regulation and increase in macrophage adherence to laminin substrata [21].

Conclusions

To harness the therapeutic potential of macrophages, it is important to elucidate the role of integrin-ligand interactions in macrophage manipulation. Integrin α2β1 can dictate macrophage function. α2β1 is a common receptor between laminin and collagen, but this commonality was not previously investigated in macrophages. Additionally, the role of IKVAV in manipulating macrophage function had not been explored prior to this work. This study established IKVAV as a macrophage manipulating peptide as it reduces M1 activation and promotes anti-inflammatory gene expression. Through agonist and antagonist experiments, the role of α2β1 was also illustrated. Blocking α2β1 reduces M1 activation by decreasing iNOS expression, and activating it increases iNOS in M2 macrophages. This may signify that α2β1 is important in dictating macrophage function when activated to M1 or M2. IKVAV was also shown to block sites provided by α2β1, although not as efficiently as an α2β1 antagonist. In the 3D hydrogel experiments, PEG-IKVAV did not have significant effects on macrophage phenotype manipulation potentially due to the concentration of IKVAV. Although reduction in iNOS is observed, manipulating IKVAV concentration and duration of

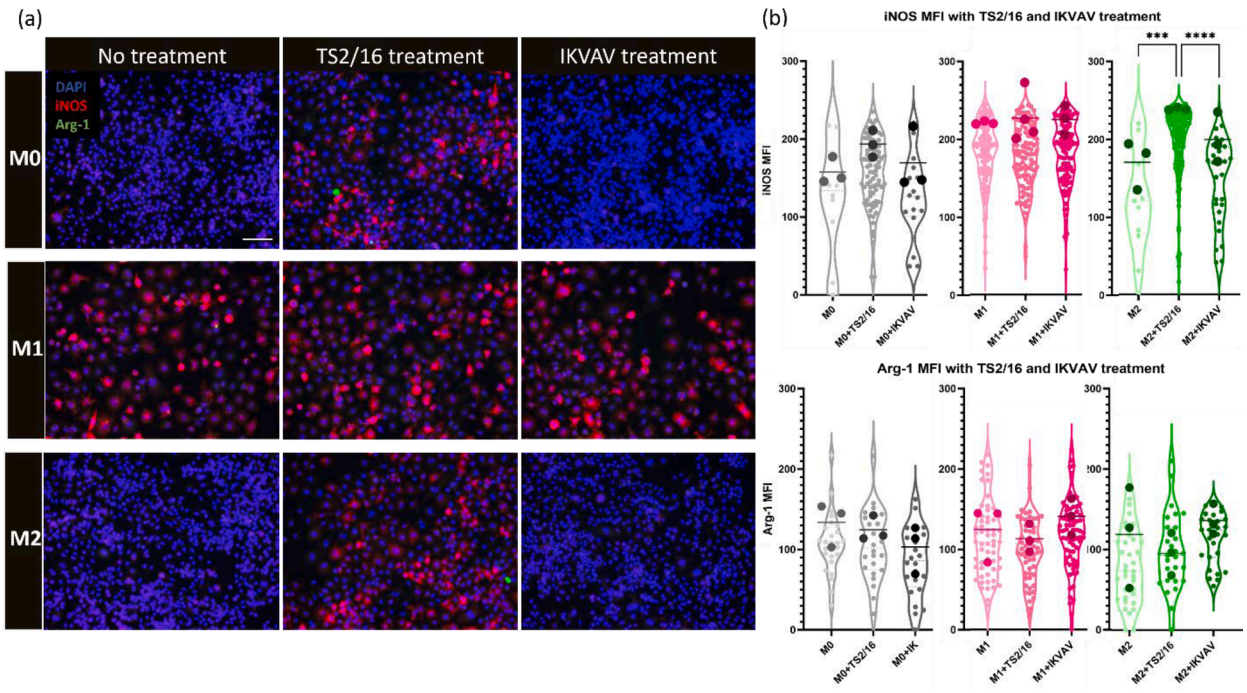

Fig. 7. Activating integrin α2β1 via agonist TS2/16 for 24 h did not affect macrophage phenotype via iNOS and Arg-1 expression. (a) Immunofluorescent stained images of M0, M1, and M2 macrophages with TS2/16 (10 μg/ml) treatment, and IKVAV (3 mM) treatment (scale = 50 mm). (b) Statistical quantification of iNOS and Arg-1 expression via MFI. Data are displayed as violin plots and each dot represents the MFI value of a cell. The larger dots represented as superplots are means of the data. One-way ANOVA with tukey's post-hoc tests compared significance between BTT-3033 and IKVAV treated groups. (n = 3; ***$p < 0.0001$, ****$p < 0.0001$).

exposure may bring forth diverging results. Thus, IKVAV can be used as a modulator for macrophages when they are activated, specifically in reducing macrophage inflammation.

Materials and methods

Cell culture and maintenance

Raw 264.7 macrophages (ATCC) were cultured in DMEM (Corning, Corning, NY) supplemented with 10 % FBS (Atlanta Biologicals, Lawrenceville, GA), 100 IU penicillin, and 100 μg/ml streptomycin (Corning). This is defined as M0 media. M0 media treated macrophages were referred to as M0 macrophages. For the polarization of macrophages to the M1 phenotype, 10 ng/ml of interferon gamma (IFNγ) (Prospec, East Brunswick, NJ) was added to M0 media with 100 ng/ml of lipopolysaccharide (LPS) (Santa Cruz Biotechnology, Dallas, TX). This is defined as M1 media and the stimulated macrophages are M1 macrophages. To obtain M2 polarized macrophages, 20 ng/mL of interleukin (IL)-4 (Prospec, East Brunswick, NJ) was added to M0 media. These macrophages were referred to as M2 macrophages. Macrophages were stimulated to the M1 and M2 phenotype 24 h post-seeding onto 24- or 48-well TCP. Macrophages were cultured for a total of 72 h with 48 h of M1 and M2 stimulation. All macrophages were maintained at 37 °C in 5 % CO_2.

Human peripheral blood derived monocytes (PBMCs) obtained from a 41-year-old Mexican/American male, purchased from Hemacare, Charles River Laboratory (#IRB202101975). The monocytes were thawed in Hanks' balanced salt solution (HBSS) without calcium or magnesium, 10 % heat inactivated human (AB) serum (Millipore Sigma, Burlington, MA), and RPMI 1640 (Fisher Scientific, Hampton, NH). The culture media for the differentiation of monocytes to macrophages was composed of RPMI 1640, 10 % heat inactivated human (AB) serum, 100 IU penicillin, and 100 μg/ml streptomycin, and macrophage colony stimulating factor (M−CSF, 20 ng/μL). Cells were plated at $0.1x10^6$ cells/mL in one 48-well for ICC, two 24-well plates for Nanostring RNA isolation, and two 6-well plates for cell encapsulation in PEG-IKVAV gels. Monocytes were incubated at 37°C with 5 % CO2 for 5 days with a media change on day 3. Monocytes were differentiated to macrophages by day 5, and subsequently polarized to M1 or M2. The M1 or classically activated macrophages were polarized with 100 ng/mL of LPS and 10 ng/mL of IFNγ, whereas the M2 or alternatively activated macrophages were polarized with 20 ng/mL of IL-4 (Prospec, East Brunswick, NJ). All macrophages were stimulated with 3 mM IKVAV and processed on day 7 for further data generation. All macrophages were either lysed in the wells to obtain RNA or fixed with 4 % paraformaldehyde for immunostaining. For the encapsulation experiments, macrophages were trypsinized for 8 min and gently scraped using a cell scraper to lift them off the wells.

IKVAV dose response in 2D

Raw 264.7 macrophages were seeded onto 48-well plates ($0.1x10^6$ cells/mL) and stimulated to M1 and M2 phenotypes 24 h post-seeding. At this time, IKVAV peptide was dissolved into the medium to identify the appropriate concentration for macrophage modulation in reducing M1 or increasing M2 activation without having significant apoptotic effects. IKVAV was added at 3 mM, 7 mM, and 10 mM concentrations in the media (n = 3 for each group with M0, M1, and M2 macrophages) and macrophages were cultured in the treatment conditions for 48 h. The soluble IKVAV treated macrophages were processed after 48 h of treatment for further analysis.

Integrin agonist and antagonist experiments with IKVAV

The antagonist was BTT-3033, a small molecule inhibitor of integrin α2β1 (Catalog no. 472410, Fisher). A dose response experiment was conducted with BTT-3033 due to its usage being more prominent in *in vivo* studies. The agonist used was TS2/16 (Catalog no. sc-53711,

Santacruz) which is a monoclonal antibody for integrin α2β1. Macrophages were seeded on day 0 and stimulated to M1 and M2 on day 1 (24 h post-seeding). At 48 h (day 2), all stimulating media was removed and replaced with BTT-3033 and TS2/16 respectively. Other groups were IKVAV treated M0, M1, and M2 macrophages to assess relations between IKVAV and α2β1.

Reverse transcription-polymerase chain reaction

Macrophages from the 2D experiment cultured in M0, M1, and M2 media with and without 3 mM IKVAV were processed at 48 h post-IKVAV treatment for RNA isolation. There was a total of 3 biological replicates. Total RNA was isolated using a TRIzol (Invitrogen) extraction method and quantified using a BioTek Synergy HT plate reader. For quantitative RT-PCR, reverse transcription occurred with 1 μg of total RNA using iScript cDNA synthesis kit (BioRAD). For uniformity in input, total RNA was normalized to the minimum concentration amongst the samples i.e. 25.44 ng/μL with 260/280 value of approximately 2.0. The parameters for RT conversion were 25 °C for 5mins, 46 °C for 20mins, and 95 °C for 1 min. Complementary DNA was amplified using SYBR Green PCR Master Mix (BioRAD) in the presence of primer sequences (IDT) using the cycling parameters as follows: 95 °C for 15 s, 60 °C for 30 s, and 72 °C for 30 s for 40 cycles. The genes used for PCR were TNFα, iNOS, IL-10, Arg-1, and the housekeeping gene was Ribosomal Protein Large P0 (RpLp0). The primer sequences are as follows: *TNFα forward: CCTGTAGCCCACGTCGTAGC, TNFα reverse: AGCAATGACTCCAAAG-TAGACC; iNOS forward: TTTGCTTCCATGCTAATGCGAAAG, iNOS reverse: GCTCTGTTGAGGTCTAAAGGCTCCG; IL-10 forward: GAGATGCCTTCAGCAGAGTGAAGA, IL-10 reverse: AGGCTTGGCAACC-CAGGTAAC; Arg-1 forward: CTCCAAGCCAAAGTCCTTAGAG, Arg-1 reverse: AGGAGCTGTCATTAGGGACATC; RpLp0 forward: AGATTCGG-GATATGCTGTTGGC, RpLp0 reverse: TCGGGTCCTAGACCAGTGTTC.* Expression levels of all genes interest were determined by normalizing genes to M0 groups. The relative fold gene expression of samples was calculated using the delta-delta cycle threshold (Ct) ($2^{-\Delta\Delta Ct}$) method.

PEG-IKVAV conjugation

IKVAV peptide (MW = 528.69 g/mol; Genscript) was conjugated to PEG by amine substitution reaction. Acrylate-PEG-succinimidyl valerate (Acryl-PEG-SVA; MW = 3400 g/mol; Laysan Bio Inc., Arab, AL) was the PEG derivative used for the substitution of SVA with the peptide. A 1.2:1 M ratio of IKVAV to PEG-SVA was mixed with 20 mM HEPBS buffer at pH 8.5, titrated to 8.0 with 0.1 M NaOH and reacted overnight at 4 ℃ under constant agitation, and protected from light. The conjugation is as previously explained [29,68,69]. The product of the reaction was acrylate-PEG-DGEA which was dialyzed with a 3.5 kDa MWCO cellulose membrane (Spectrum Laboratories) to permeate the unconjugated molecules. The final solution was then lyophilized (Labonco, Kansas City, MO) and stored at −80 °C until use. A working concentration of 3 mM was determined appropriate for cell instruction as assessed by the dose response study. Other components conjugated were Arg-Gly-Asp-Ser (RGDS; MW = 433.42 g/mol) to PEG for cell adhesion at 1.2:1 M ratio, and GGGPQGIWGQGK (PQ) to PEG for cell-mediated degradation at 1:2 M ratio.

Encapsulation of cells within PEG-IKVAV hydrogels

Macrophages were encapsulated in two different hydrogel groups – control and experimental (PEG-IKVAV). Herein, the control hydrogels were designed with 3.5 mM PEG-RGDS and 20 % w/v PEG-PQ-PEG. The experimental or PEG-IKVAV hydrogels consisted of PEG-RGDS, PEG-PQ-PEG and 3 mM PEG-IKVAV.

To form the hydrogels, the covalently conjugated macromers were dissolved in HEPES buffered saline (HBS; 10 mM HEPES; and 100 mM NaCl at pH 7.4) with 1.5 % TEOA (Sigma). Eosin Y (10 μM), a photoinitiator, and 0.35 % N-Vinylpyrrolidone (NVP) were also mixed with the macromers solutions. The appropriate cell count was added to the mixture as well ($10x10^6$ cells/mL). A 5 μL volume of the macrophages and polymer solution was pipetted onto a polydimethylsiloxane (PDMS) slab with two PDMS spacers (385 μm thick) to allow for the 3D hydrogel formation. The drop was exposed to white light for 60 s under a methacrylated coverslip. The methacrylated coverslip allowed for the acrylate groups to attached onto the coverslip and prevent dislodging of the hydrogel. White light exposure activated eosin Y, leading to free radical generation. The hydrophobic acrylate groups converged into micelle-like centers and the free radicals propagated into a crosslinked network. Rapid polymerization of the hydrogel occurred under white light with no harmful exposure to the encapsulated cells. The hydrogel was then placed in 24 or 48-well plates and media was gently pipetted into wells.

Immunostaining

All immunofluorescence staining experiments were fixed in 4 % paraformaldehyde for 20–25 mins in 2D or 45 mins in 3D. The samples from the soluble IKVAV studies (2D) were fixed at 48 h post-stimulation and IKVAV treatment. The samples from the PEG-IKVAV encapsulation study (3D) were fixed at 48 h post-M1/M2 stimulation but 72 h post-encapsulation. Permeabilization of the cell membrane occurred by exposing to 0.125 % Triton-X for 10mins (2D) or 0.25 % Triton-X for 45mins (3D) at room temperature (RT), followed by rinses with TBS. Blocking was induced in the presence of 5 % DS for 3 h (2D) or overnight (3D) at 4 °C, followed by TBS rinses. Primary antibody incubation occurred overnight for both 2D and 3D samples. The primary antibodies utilized in this work were diluted in 0.5 % DS and are as listed: iNOS (1:200; Rabbit Anti-Mouse Polyclonal Antibody; Catalog no. PA3-030A; Invitrogen, Waltham, MA); Arg-1 (1:200; Mouse Anti-Mouse monoclonal antibody; Catalog no. 66129–1-Ig; Proteintech, Rosemont, IL); Integrin β1/ITGB1 Antibody (TS2/16) (1:200; Mouse Anti-Mouse monoclonal antibody; Catalog no. sc-53711; Santa Cruz Biotechnology Inc., Dallas, TX). Rinses occurred 5 or 6 times in 0.01 % Tween in TBS for 20 mins (2D) or 90–120 mins (3D), with the except of the last rinse being in TBS only. The samples were then incubated in secondary antibodies overnight at 4 °C- Alexa Fluor 555 Donkey Anti-Rabbit for iNOS (1:200; Catalog no. PIA32794; Thermofisher, Waltham, MA); Alexa Fluor 488 Donkey Anti-Mouse for Arg-1 (1:200; Catalog no. A-21202; Thermofisher, Waltham, MA); Alexa Fluor 555 Donkey Anti-Mouse for TS2/16 (1:200; Catalog no. A-31570; Thermofisher, Waltham, MA). The rinse after secondary antibody incubation was an hour long in TBS. Cell nuclei were stained with 2 μM DAPI (Catalog no. 10236276001; Sigma Aldrich, St. Louis, MO) followed by two rinses with TBS for 5mins each.

Imaging and image analysis

Images were captured on the Keyence BZ-X800 microscope. Images were quantified assessing mean fluorescence intensity (MFI) and by counting total cell count per view field for $DAPI^+$ cells to ensure equal comparison. The violin charts in figures obtained from MFI calculations of each cell accounted for the shift in fluorescence intensity of a population of stained macrophages and enabled quantification of overall expression. The violin plots are charted in a way that only the cells that are positively expressing the marker of interest (in this case iNOS or Arg-1) are being included as a point. Additionally, the violin charts are represented as Superplots of data. Herein, the smaller lighter colored dots are $DAPI^+$ cells that are positively expressing the marker of interest, and the larger darker colored dots are the means of the data. Five images were taken per well in 2D or per hydrogel in 3D. Images from the hydrogel were captured as single frames or 15 μm Z-stacks which were projected onto a single plane using ImageJ. In a random unbiased manner, an image was selected from each biological replicate (n = 6). The overlay of the image was imported into ImageJ and split across each

channel using the 'Color > Split channels' function. The result was 3 grayscale images for the blue (DAPI) channel, red (iNOS; BTT-3033; TS2/16) channel, and green (Arg-1) channel. Each grayscale 8-bit image was then thresholded manually. The size range was 0.001-Infinity for each image. DAPI count was quantified using the 'automated cell counting of single color image' feature and saved into an excel sheet. The MFI for each image was calculated after thresholding, using the 'Analyze particles' function. Measurements were set preemptively using 'Analyze > Set Measurements' and checking area, mean grey value and standard deviation. After setting measurements, the'Analyze particles' function was used again with the 'Add to Manager' function checked. This displays the region of interest (ROI) manager wherein each cell is listed. On selecting all the cells listed, the fluorescence intensity can then be measured. The values were exported into an excel file. The mean grey value from the table is the fluorescence intensity measured. All relevant values were exported into GraphPad Prism for further statistical analyses. The representative fluorescent images were overlays of stained macrophages.

Nanostring gene expression analysis

Human monocyte derived macrophages, treated with 3 mM IKVAV peptide and stimulated to M1/M2, were assessed for gene expression profiles through the Nanostring nCounter Sprint. RNA was lysed directly in the wells and combined to obtain maximal RNA material on isolation. RNA isolation occurred following manufacturer's protocol using the Qiagen RNeasy Plus Micro Kit and stored at −80 °C until use. Yield quantification was obtained by a BioTek Synergy HT plate reader with acceptable concentrations of more than 10 ng/μL and 260/280 value of approximately 2.0. RNA concentrations were diluted to a common input of 50 ng (10 ng/μL) per sample. The nCounter Myeloid Innate Immunity V2 panel was utilized for the experiment. Following instructions provided by the manufacturer for using the Nanostring nCounter Sprint, a master mix was created with the reporter probe set, hybridization buffer, samples, and capture probe set. Two biological replicates were loaded into the 12-panel cartridge making a total of 6 samples, i.e., M0, M1, and M2 macrophages with and without IKVAV treatment. In addition to 2 biological replicates, there were 4 technical replicates, wherein each well was a technical replicate. Each lane in the Nanostring panel consists of negative controls, positive controls and housekeeping genes, thus each lane is assessed independently for quality control. Nanostring data were first normalized to internal positive and negative controls and subsequently normalized to the geometric mean of all the housekeeping genes inbuilt in panel. Pathways were analyzed from the annotated gene set global significance score, calculated as the square root of the mean squared t-statistics of genes. The gene expression profile of human monocyte derived macrophages on IKVAV treatment was evaluated. The threshold of corrected p-values less than 0.5 was set as per the recommendation on the analysis software. The volcano plot was rendered by the Advanced Analysis software in Nanostring. Log2 fold change differences were plotted in GraphPad Prism using the row Z score of log-transformed normalized data.

Statistical analyses

Images were quantified by MFI across all groups or total cell count per view field for $DAPI^{+}$ cells. The software used for all statistical quantification was GraphPad Prism. To obtain statistical significance, one-way ANOVA with Tukey's post-hoc comparison tests were performed for all 2D and 3D experiments. MFI is represented in arbitrary units (a.u.) with standard deviation (SD) as violin plots where each dot represents a cell. RT-PCR was quantified by one-way ANOVA with M0 as the control group normalized to RpLp0. The fold change gene expression values are represented. All statistics were displayed as mean ± standard deviation (SD) and significance was determined by $p < 0.05$. Nanostring data were evaluated by forming a volcano plot. The volcano plot was generated by conducting a pathway analysis from the annotated gene set global significance score, calculated as the square root of the mean squared t-statistics of genes. The volcano plot was rendered by plotting log2 fold change values against negative log 10 of the p values. Genes to the left of the baseline are downregulated with IKVAV treatment and genes to the right are upregulated with IKVAV treatment. Heatmaps and bar plots were formed sequestering genes of interest for better visualization.

CRediT authorship contribution statement

Aakanksha Jha: Conceptualization, Data curation, Formal analysis, Investigation, Methodology, Software, Validation, Visualization, Writing – original draft, Writing – review & editing. **Erika Moore:** Funding acquisition, Methodology, Project administration, Resources, Supervision, Validation, Writing – review & editing.

Declaration of competing interest

The authors declare the following financial interests/personal relationships which may be considered as potential competing interests: Erika Moore reports a relationship with National Science Foundation that includes: funding grants. If there are other authors, they declare that they have no known competing financial interests or personal relationships that could have appeared to influence the work reported in this paper.

Data availability

Data will be made available on request.

Acknowledgements

This work was financially supported in part by the Rhines Rising Star Larry Hench Professorship (E.M.) and NSF Career Grant #2237741. Under #IRB202101975 through the University of Florida Institutional Review Board, the authors purchased human monocytes to profile the human macrophage response to IKVAV peptide.

The authors would like to thank Nana Owusu-Boaitey and Alison Veintimilla for their valuable feedback during the writing process.

Appendix A. Supplementary data

Supplementary data to this article can be found online at https://doi.org/10.1016/j.mbplus.2024.100143.

References

[1] B. Yue, Biology of the extracellular matrix: an overview, J. Glaucoma 23 (2014) S20–S23.
[2] R.O. Hynes, A. Naba, Overview of the matrisome–an inventory of extracellular matrix constituents and functions, Cold Spring Harb. Perspect. Biol. 4 (2012) a004903–a004903.
[3] E.F. Plow, T.A. Haas, L. Zhang, J. Loftus, J.W. Smith, Ligand Binding to Integrins, J. Biol. Chem. 275 (2000) 21785–21788.
[4] Y. Takada, X. Ye, S. Simon, The integrins, Genome Biol. 8 (2007), 215–215.
[5] B. Alberts, J.A. Lewis et al. Integrins. in *Molecular Biology of the Cell* (Garland Science, 2002).
[6] E.H.J. Danen. Integrins: An Overview of Structural and Functional Aspects. in *Madame Curie Bioscience Database*.
[7] R.O. Hynes, Integrins: Bidirectional, Allosteric Signaling Machines, Cell 110 (2002) 673–687.
[8] C.D. Reyes, T.A. Petrie, A.J. García, Mixed extracellular matrix ligands synergistically modulate integrin adhesion and signaling, J. Cell. Physiol. 217 (2008) 450–458.
[9] R. Timpl, et al., Laminin–a glycoprotein from basement membranes, J. Biol. Chem. 254 (1979) 9933–9937.
[10] V. Kumar. Macrophages: The Potent Immunoregulatory Innate Immune Cells. in *Macrophage Activation* (ed. Bhat, K. H.) (IntechOpen, 2019). doi:10.5772/intechopen.88013.

[11] S. Epelman, K.J. Lavine, G.J. Randolph, Origin and functions of tissue macrophages, Immunity 41 (2014) 21–35.
[12] D. Hirayama, T. Iida, H. Nakase, The Phagocytic Function of Macrophage-Enforcing Innate Immunity and Tissue Homeostasis, Int. J. Mol. Sci. 19 (2017).
[13] G. Sreejit, A.J. Fleetwood, A.J. Murphy, P.R. Nagareddy, Origins and diversity of macrophages in health and disease, Clin. Transl. Immunol. 9 (2020) e1222–e1222.
[14] P.J. Murray, et al., Macrophage Activation and Polarization: Nomenclature and Experimental Guidelines, Immunity 41 (2014).
[15] F.O. Martinez, S. Gordon, The M1 and M2 paradigm of macrophage activation: Time for reassessment, F1000Prime Rep. (2014), 10.12703/P6-13.
[16] M.J. Davis, *et al.* Macrophage M1/M2 polarization dynamically adapts to changes in cytokine microenvironments in Cryptococcus neoformans infection. *mBio* (2013) doi:10.1128/mBio.00264-13.
[17] E.J. Hoffmann, S.M. Ponik, Biomechanical Contributions to Macrophage Activation in the Tumor Microenvironment, Front. Oncol. 10 (2020) 787.
[18] F.Y. McWhorter, C.T. Davis, W.F. Liu, Physical and mechanical regulation of macrophage phenotype and function, Cell. Mol. Life Sci. CMLS 72 (2015) 1303–1316.
[19] C.E. Witherel, et al., Regulation of extracellular matrix assembly and structure by hybrid M1/M2 macrophages, Biomaterials 269 (2021) 120667.
[20] A.M. Mercurio, L.M. Shaw, Macrophage interactions with laminin: PMA selectively induces the adherence and spreading of mouse macrophages on a laminin substratum, J. Cell Biol. 107 (1988) 1873–1880.
[21] T.K. Huard, H.L. Malinoff, M.S. Wicha, Macrophages express a plasma membrane receptor for basement membrane laminin, Am. J. Pathol. 123 (1986) 365–370.
[22] M. Li, Q. Hou, L. Zhong, Y. Zhao, X. Fu, Macrophage Related Chronic Inflammation in Non-Healing Wounds, Front. Immunol. 12 (2021).
[23] A.G. Arroyo, M.L. Iruela-Arispe, Extracellular matrix, inflammation, and the angiogenic response, Cardiovasc. Res. 86 (2010) 226–235.
[24] A.M. Mercurio, Lessons from the alpha2 integrin knockout mouse, Am. J. Pathol. 161 (2002) 3–6.
[25] B.H. Cha, et al., Integrin-Mediated Interactions Control Macrophage Polarization in 3D Hydrogels, Adv. Healthc. Mater. (2017), https://doi.org/10.1002/adhm.201700289.
[26] M.C. Zweers, et al., Integrin α2β1 Is Required for Regulation of Murine Wound Angiogenesis but Is Dispensable for Reepithelialization, J. Invest. Dermatol. 127 (2007) 467–478.
[27] J. Emsley, C.G. Knight, R.W. Farndale, M.J. Barnes, R.C. Liddington, Structural Basis of Collagen Recognition by Integrin α2β1, Cell 101 (2000) 47–56.
[28] L.R. Languino, et al., Endothelial cells use alpha 2 beta 1 integrin as a laminin receptor, J. Cell Biol. 109 (1989) 2455–2462.
[29] A. Jha, E. Moore, Collagen-derived peptide, DGEA, inhibits pro-inflammatory macrophages in biofunctional hydrogels, J. Mater. Res. 37 (2022) 77–87.
[30] K. Tashiro, et al., A Synthetic Peptide Containing the IKVAV Sequence from the A Chain of Laminin Mediates Cell Attachment, Migration, and Neurite Outgrowth, J. Biol. Chem. 264 (1989) 16174–16182.
[31] S. Ali, J.E. Saik, D.J. Gould, M.E. Dickinson, J.L. West, Immobilization of Cell-Adhesive Laminin Peptides in Degradable PEGDA Hydrogels Influences Endothelial Cell Tubulogenesis, BioResearch Open Access 2 (2013) 241–249.
[32] T.H. Perera, X. Lu, L.A. Smith Callahan, Effect of Laminin Derived Peptides IKVAV and LRE Tethered to Hyaluronic Acid on hiPSC Derived Neural Stem Cell Morphology, Attachment and Neurite Extension. *J. Funct. Biomater.* 11 (2020).
[33] M. Nakamura, et al., Promotion of Angiogenesis by an Artificial Extracellular Matrix Protein Containing the Laminin-1-Derived IKVAV Sequence, Bioconjug. Chem. 20 (2009) 1759–1764.
[34] L.E. Hind, E.B. Lurier, M. Dembo, K.L. Spiller, D.A. Hammer, Effect of M1–M2 Polarization on the Motility and Traction Stresses of Primary Human Macrophages, Cell. Mol. Bioeng. 9 (2016), 455–455.
[35] Z. Strizova, et al., M1/M2 macrophages and their overlaps – myth or reality? Clin. Sci. Lond. Engl. 1979 (137) (2023) 1067–1093.
[36] M. Rath, I. Müller, P. Kropf, E.I. Closs, M. Munder, Metabolism via arginase or nitric oxide synthase: Two competing arginine pathways in macrophages, Front. Immunol. 5 (2014), 532–532.
[37] K.D. Kröncke, K. Fehsel, V. Kolb-Bachofen, Inducible nitric oxide synthase in human diseases, Clin. Exp. Immunol. 113 (1998), 147–147.
[38] S.C. Funes, M. Rios, J. Escobar-Vera, A.M. Kalergis, Implications of macrophage polarization in autoimmunity, Immunology 154 (2018) 186–195.
[39] Z. Yang, X.-F. Ming, Functions of arginase isoforms in macrophage inflammatory responses: impact on cardiovascular diseases and metabolic disorders, Front. Immunol. 5 (2014), 533–533.
[40] T.A. Wynn, K.M. Vannella, Macrophages in Tissue Repair, Regeneration, and Fibrosis, Immunity 44 (2016) 450–462.
[41] H. Hosseinkhani, et al., Engineering three-dimensional collagen-IKVAV matrix to mimic neural microenvironment, ACS Chem. Neurosci. 4 (2013) 1229–1235.
[42] J. Zeng, C. Gu, Y. Sun, X. Chen, Engineering of M2 Macrophages-Derived Exosomes via Click Chemistry for Spinal Cord Injury Repair, Adv. Healthc. Mater. 12 (2023) 2203391.
[43] F. Bonnefoy, et al., Factors Produced by Macrophages Eliminating Apoptotic Cells Demonstrate Pro-Resolutive Properties and Terminate Ongoing Inflammation, Front. Immunol. 9 (2018) 2586.
[44] M. Lohela, M. Bry, T. Tammela, K. Alitalo, VEGFs and receptors involved in angiogenesis versus lymphangiogenesis, Curr. Opin. Cell Biol. 21 (2009) 154–165.
[45] B. Zhang, et al., Gene expression of vascular endothelial growth factor A and hypoxic adaptation in Tibetan pig, J. Anim. Sci. Biotechnol. 7 (2016) 21.
[46] R. Walczak, et al., Transcription of the Vascular Endothelial Growth Factor Gene in Macrophages Is Regulated by Liver X Receptors*, J. Biol. Chem. 279 (2004) 9905–9911.
[47] G. Grieb, M. Merk, J. Bernhagen, R. Bucala, Macrophage migration inhibitory factor (MIF): a promising biomarker, Drug News Perspect. 23 (2010) 257–264.
[48] S. Han, et al., Macrophage insulin receptor deficiency increases ER stress-induced apoptosis and necrotic core formation in advanced atherosclerotic lesions, Cell Metab. 3 (2006) 257–266.
[49] Y. Yang, et al., Functional Roles of p38 Mitogen-Activated Protein Kinase in Macrophage-Mediated Inflammatory Responses, Mediators Inflamm. 2014 (2014) 352371.
[50] CCRL2 promotes antitumor T-cell immunity via amplifying TLR4-mediated immunostimulatory macrophage activation | PNAS. https://www.pnas.org/doi/10.1073/pnas.2024171118.
[51] M. Takahashi, et al., Macrophage lipoprotein lipase modulates the development of atherosclerosis but not adiposity, J. Lipid Res. 54 (2013) 1124–1134.
[52] Y. Liu, et al., Cell Surface Receptor FPR2 Promotes Antitumor Host Defense by Limiting M2 Polarization of Macrophages, Cancer Res. 73 (2013) 550–560.
[53] S. Hörber, et al., The Atypical Inhibitor of NF-κB, IκBζ, Controls Macrophage Interleukin-10 Expression, J. Biol. Chem. 291 (2016) 12851–12861.
[54] Y. Cheng, et al., Gelsolin Inhibits the Inflammatory Process Induced by LPS, Cell. Physiol. Biochem. 41 (2017) 205–212.
[55] Y. Kikkawa, et al., Laminin-111-derived peptides and cancer, Cell Adhes. Migr. 7 (2013) 150–159.
[56] C. Li, et al., Critical role and its underlying molecular events of the plasminogen receptor, S100A10 in malignant tumor and non-tumor diseases, J. Cancer 11 (2020) 826–836.
[57] A. Jha, J. Larkin III, E. Moore, SOCS1-KIR Peptide in PEGDA Hydrogels Reduces Pro-Inflammatory Macrophage Activation, Macromol. Biosci. 23 (2023) 2300237.
[58] S.L. Bellis, Advantages of RGD peptides for directing cell association with biomaterials, Biomaterials 32 (2011), 4205–4205.
[59] M.A. Arnaout, B. Mahalingam, J.-P. Xiong, Integrin Structure, Allostery, and Bidirectional Signaling, Annu. Rev. Cell Dev. Biol. 21 (2005) 381–410.
[60] B. Li, et al., IKVAV regulates ERK1/2 and Akt signalling pathways in BMMSC population growth and proliferation, Cell Prolif. 47 (2014) 133–145.
[61] L. Nissinen, et al., Novel α2β1 integrin inhibitors reveal that integrin binding to collagen under shear stress conditions does not require receptor preactivation, J. Biol. Chem. 287 (2012) 44694–44702.
[62] L. Nissinen, et al., Sulfonamide inhibitors of α2β1 integrin reveal the essential role of collagen receptors in in vivo models of inflammation, Pharmacol. Res. Perspect. 3 (2015) e00146–e00146.
[63] S.M. Jung, M. Moroi, Activation of the Platelet Collagen Receptor Integrin α2β1: Its Mechanism and Participation in the Physiological Functions of Platelets, Trends Cardiovasc. Med. 10 (2000) 285–292.
[64] V.M. Freitas, et al., SIKVAV, a laminin alpha1-derived peptide, interacts with integrins and increases protease activity of a human salivary gland adenoid cystic carcinoma cell line through the ERK 1/2 signaling pathway, Am. J. Pathol. 171 (2007) 124–138.
[65] T. Maeda, K. Titani, K. Sekiguchi, Cell-adhesive activity and receptor-binding specificity of the laminin-derived YIGSR sequence grafted onto Staphylococcal protein A, J. Biochem. (tokyo) 115 (1994) 182–189.
[66] K.M. Khan, D.J. Falcone, Selective activation of MAPK(erk1/2) by laminin-1 peptide alpha1:Ser(2091)-Arg(2108) regulates macrophage degradative phenotype, J. Biol. Chem. 275 (2000) 4492–4498.
[67] S.M. Jung, M. Moroi, Platelets interact with soluble and insoluble collagens through characteristically different reactions, J. Biol. Chem. 273 (1998) 14827–14837.
[68] Y. Wu, K.J. Grande-Allen, J.L. West, Adhesive Peptide Sequences Regulate Valve Interstitial Cell Adhesion, Phenotype and Extracellular Matrix Deposition, Cell. Mol. Bioeng. 9 (2016), 479–479.
[69] E.M. Moore, et al., Macrophages Influence Vessel Formation in 3D Bioactive Hydrogels, Adv. Biosyst. 1 (2017), 1600021–1600021.